

Effects of receiver diversity on bit error rate of underwater optical wireless communication systems in weak oceanic turbulence

Gökçe, Muhsin Caner; Baykal, Yahya; Ata, Yalçın

DOI

[10.1007/s11107-025-01032-z](https://doi.org/10.1007/s11107-025-01032-z)

Publication date

2025

Document Version

Final published version

Published in

Photonic Network Communications

Citation (APA)

Gökçe, M. C., Baykal, Y., & Ata, Y. (2025). Effects of receiver diversity on bit error rate of underwater optical wireless communication systems in weak oceanic turbulence. *Photonic Network Communications*, 50(2), Article 2. <https://doi.org/10.1007/s11107-025-01032-z>

Important note

To cite this publication, please use the final published version (if applicable). Please check the document version above.

Copyright

Other than for strictly personal use, it is not permitted to download, forward or distribute the text or part of it, without the consent of the author(s) and/or copyright holder(s), unless the work is under an open content license such as Creative Commons.

Takedown policy

Please contact us and provide details if you believe this document breaches copyrights. We will remove access to the work immediately and investigate your claim.

**Green Open Access added to [TU Delft Institutional Repository](#)
as part of the Taverne amendment.**

More information about this copyright law amendment
can be found at <https://www.openaccess.nl>.

Otherwise as indicated in the copyright section:
the publisher is the copyright holder of this work and the
author uses the Dutch legislation to make this work public.



Effects of receiver diversity on bit error rate of underwater optical wireless communication systems in weak oceanic turbulence

Muhsin Caner Gökçe^{1,4} · Yahya Baykal² · Yalçın Ata³

Received: 10 April 2022 / Accepted: 23 July 2025

© The Author(s), under exclusive licence to Springer Science+Business Media, LLC, part of Springer Nature 2025

Abstract

The receiver spatial diversity techniques are employed in underwater optical wireless communication (OWC) systems to mitigate oceanic turbulence, improving the bit error rate performance. In this paper, we consider an OWC system employing a binary phase-shift keying (BPSK) modulated Gaussian beam at the transmitter and employing receiver spatial diversity at the receiver. The techniques for receiver spatial diversity systems considered in the study are selection combining (SC), equal gain combining (EGC), and the maximum ratio combining (MRC). The bit error rate (BER) performance of the OWC system operating in weak oceanic turbulence is investigated by calculating the Gaussian beam's turbulence-induced scintillation index and the received optical intensity. It is found that the receiver spatial diversity techniques, especially EGC and MRC, are very effective for reducing the BER of an OWC system in weak oceanic turbulence. Furthermore, the BER performance of the underwater OWC system sees an improvement with an increase in the number of photodetectors or a decrease in the level of oceanic turbulence. Moreover, an improvement in the photodetector responsivity or a reduction in the system's noise factor contributes to achieving a favorable BER performance.

Keywords Underwater optical wireless communication · Receiver spatial diversity · Optical wave propagation · Binary phase-shift keying · Scintillation index · Weak oceanic turbulence

1 Introduction

The recent demands for high data rates for underwater applications such as real-time video transmission, ocean monitoring, marine archeology, and sensor networks make underwater optical wireless communications (OWC) systems attractive and induce development in easy to install commercial OWC products [1–4]. The visible light sources such as laser diodes (LD) or light-emitting diodes (LEDs)

used in an underwater OWC system can provide data rates in the order of Gbps, but unfortunately, the performances of such systems are currently limited to short link ranges of 10–150 m because of the physical nature of oceanic water which highly absorbs and scatters the transmitted optical signals [2, 5]. The degradation effects of absorption and scattering in clear ocean are relatively weaker for optical waves having the wavelengths range of 450–550 nm; however, serious distortions on the transmitted signal are sensed in harbor water in which the amplitude of the transmitted signal attenuates one-tenth in a meter and also inter-symbol interference (ISI) occurs. Another degradation effect of oceanic water is oceanic turbulence which distorts the propagation properties of the laser beam, resulting in degradations in the OWC system performance [6, 7]. Oceanic turbulence occurs due to random fluctuations in the refractive index of the seawater, and the well-known degradation effects of oceanic turbulence on the propagating optical wave are turbulence-induced scintillation and beam spreading. Due to the scintillation effect, the intensity of the transmit signal fluctuates causing false detection at the receiver. On the other hand, the beam spreading results in attenuation in the received

✉ Muhsin Caner Gökçe
muhsin.gokce@tedu.edu.tr

¹ Department of Electrical and Electronics Engineering, TED University, Ziya Gökalp Cad. No: 47-48, Kolej Çankaya, 06420 Ankara, Turkey

² Department of Electrical-Electronics Engineering, Çankaya University, Yukarıyurtçu Mah. Mimar Sinan Cad. No: 4, Etimesgut, 06790 Ankara, Turkey

³ Electrical and Electronics Engineering, OSTIM Technical University, OSTIM, 06374 Ankara, Turkey

⁴ Department of Geoscience and Remote Sensing, Delft University of Technology, 2628CD Delft, Netherlands

intensity causing a decrease in the receiver signal-to-noise ratio (SNR) and thus reducing the bit error rate (BER) performance. Overall, the attenuation in received intensity and the optical scintillation become important factors determining the performance of such communication systems and have been analyzed in several types of studies [6–10] with the help of an accurate oceanic power spectrum model defined by Nikishov and Nikishov [11]. In [8], the aperture averaged scintillation index and the BER of a Gaussian beam propagating in weak oceanic turbulence have been reported. In [9], the scintillation index formula has been derived under the assumption of spherical and the plane wave propagation. In [10], the scintillation index and BER for a focused Gaussian beam have been analyzed in weak oceanic turbulence.

There are various techniques applied in OWC systems to mitigate the effect of oceanic turbulence, such as adaptive optics [12, 13], beam shaping [14], and modulation [13, 15, 16]. Furthermore, spatial diversity techniques are used for efficient turbulence mitigation tools that can be applied both at the transmitter and receiver. In the literature, several works have been documented in [17–25] studying spatial diversity effects on the performance of OWC systems in underwater. In [17], the theoretical exact BER expression for spatial diversity system with DC-biased optical orthogonal frequency division multiplexing (DCO-OFDM) is derived for weak oceanic turbulence, and the numerical simulations are supported by the derived expression. A similar experimentally supported study has been reported for clear and coastal water [18]. The closed-form BER expressions for an underwater OWC system employing transmit, receive, and transmit/receive diversities with channel coding techniques are obtained in [19]. The comprehensive studies including the effects of spatial diversity, absorption scattering, and weak oceanic turbulence on the BER performance of an underwater OWC system are presented in [20–22]. The effects of spatial diversity together with ISI, multi-pulse position modulation on the BER performance of an underwater OWC system under the effect of oceanic turbulence are reported [23]. An experimental demonstration of a multiple-input multiple-output (MIMO) OFDM OWC system with BER simulations is examined in [24]. Finally, in [25], the authors report how the transmit diversity reduces the scintillation and the resulting BER in weak oceanic turbulence.

It is worth mentioning that a recently conducted experimental study, highlighting the ingenuity of applying MRC in the underwater optical wireless communication (UOWC) system, has been documented in reference [26]. The outcomes of experiments presented in reference [26] demonstrate that spatial diversity can guarantee favorable performance in terms of BER and outage probability when employing MRC in correlated turbulence channels. In addition, analytical formulations for the average symbol error probability (SEP) and average channel capacity are

introduced for optical waves propagating through oceanic turbulence using M-ary pulse position modulation (PPM), subject to constraints on limited average power and peak power [27]. Furthermore, the evaluation of channel capacity for UOWC systems is undertaken, considering the effects of inter-symbol interference (ISI) and salinity-induced oceanic turbulence [28]. This analysis assumes a precise representation of the undersea optical channel, achieved through the linear discrete-time filtering of the input symbols, as outlined in reference [28].

In this paper, we use receiver spatial diversity techniques, namely, selection combining (SelC), equal gain combining (EGC), and maximum ratio combining (MRC) to mitigate the effect of oceanic turbulence and investigate their effects on the BER performance of underwater OWC systems. For this reason, considering the propagation of BPSK modulated Gaussian beam in weak oceanic turbulence, we evaluate the turbulence-induced scintillation index with the help of the Rytov theory, the turbulence-induced received optical intensity with the help of the extended Huygens–Fresnel principle, and calculate the resulting BER values for the log-normal channel under the influence of various signal noises in underwater. It should be noted that we have previously reported the BER performances of BPSK modulated Gaussian beam in anisotropic and weak oceanic turbulence [15, 16]. However, in this work, we focus on the effects of spatial diversity on the system performance.

The rest of the paper is organized as follows: In section II, we present the analytical formulas to evaluate the Gaussian beam's received optical intensity and the scintillation index, which are used for the evaluation of BER of an OWC system employing SelC, MRC, and EGC under the effect of various underwater noises and oceanic turbulence levels. In section III, we present numerical results for the BER investigations of an OWC system operating in weak oceanic turbulence. Finally, we give conclusions in section IV.

2 Formulation

2.1 Power spectrum of oceanic turbulence fluctuations

Nikishov's power spectrum [11] is commonly preferred in analyzing optical wave propagation in oceanic turbulence and has important consequences on various aspects of optical wave propagation through the ocean such as change in the mean field and irradiance, spot size (i.e., footprint of the received optical beam), beam wander, and particularly scintillation. The power spectrum model for refractive index fluctuations of isotropic and homogeneous oceanic water that is based on

salinity, temperature, and coupling fluctuations is represented by [11]

$$\Phi(\kappa) = 0.388 \times 10^{-8} \kappa^{-11/3} \varepsilon^{-1/3} [1 + 2.35(\kappa\eta)^{2/3}] \frac{X_T}{\omega^2} (\omega^2 e^{-A_T \delta} + e^{-A_S \delta} - 2\omega e^{-A_{TS} \delta}), \tag{1}$$

where κ is the spatial frequency, ε is the rate of dissipation of kinetic energy per unit mass of fluid, η is the Kolmogorov microscale (inner scale), X_T is the rate of dissipation of mean-squared temperature, and ω is a unitless parameter providing the ratio of temperature to salinity contributions to the refractive index spectrum, $A_T = 1.863 \times 10^{-2}$, $A_S = 1.9 \times 10^{-4}$, $A_{TS} = 9.41 \times 10^{-3}$, and $\delta(\kappa, \eta) = 8.284(\kappa\eta)^{4/3} + 12.978(\kappa\eta)^2$. It should be noted that η varies in the range of $0.01 - 6 \times 10^{-5}$ m, and ε varies in the range of $10^{-10} - 10^{-1} \text{m}^2/\text{s}^3$, depending on the layers of ocean (abyssal ocean to most actively turbulent region, i.e., near ocean surface). In a similar fashion, X_T ranges from $10^{-10} \text{K}^2/\text{s}$ to $10^{-4} \text{K}^2/\text{s}$, and the unitless parameter ω is a crucial parameter since it emphasizes the relative strength of temperature and salinity fluctuations, ω ranges from -5 dominating temperature-induced turbulence to 0 dominating salinity-induced turbulence [6, 7].

2.2 Gaussian beam propagation through oceanic turbulence

2.2.1 Received optical intensity

The beam field of the Gaussian source laser at the transmitter spatial plane is given by [8]

$$u(\mathbf{s}) = A_s \exp \left[-\frac{1}{2} k \left(\frac{1}{k\alpha_s^2} + \frac{i}{F_0} \right) \mathbf{s}^2 \right] \tag{2}$$

where A_s is the field amplitude, $k = 2\pi/\lambda$ is the wavenumber, α_s is the laser source size, $i = \sqrt{-1}$, λ is the wavelength, $\mathbf{s} = (s_x, s_y)$ denotes the source transverse coordinates, and F_0 is the phase front radius of curvature. In this study, F_0 is chosen as infinity to represent the collimated beam. To find the received average optical intensity on the axis, we use the extended Huygens–Fresnel principle in Eq. (3) which involves the convolution of source field Eq. (2) with the spherical wave response of the turbulent medium [25], which is

$$\langle I(z = L) \rangle = \frac{1}{(\lambda L)^2} \int_{-\infty}^{\infty} \int_{-\infty}^{\infty} \int_{-\infty}^{\infty} \int_{-\infty}^{\infty} \mathbf{d}\mathbf{s}_1 \mathbf{d}\mathbf{s}_2 u(\mathbf{s}_1) u^*(\mathbf{s}_2) \times \exp \left\{ \frac{ik}{2L} \left[(\mathbf{s}_1)^2 - (\mathbf{s}_2)^2 \right] - \rho_0^{-2} (\mathbf{s}_1 - \mathbf{s}_2)^2 \right\} \tag{3}$$

where L is link distance, $*$ is the complex conjugate, and ρ_0 is the coherence length of the spherical wave propagating

through the ocean, which is given by [29, 30]

$$\rho_0 = \left[\frac{\pi^2 k^2 L}{3} \int_0^\infty \kappa^3 \Phi(\kappa) d\kappa \right]^{-1/2} = [1.28 \times 10^{-8} k^2 L \eta^{-1/3} \varepsilon^{-1/3} X_T (6.78 + 47.57 w^{-2} - 17.67 w^{-1})]^{-1/2} \tag{4}$$

Inserting the source field Eq. (2) into the convolutional integral, Eq. (3), and solving Eq. (3) by the repeated use of Eq. (3.323.2) of [31], we find the average received optical intensity underwater [32] as follows:

$$\langle I(z = L) \rangle = \frac{A_s^2 \left(\frac{k\alpha_s}{2L} \right)^2}{\left(\frac{1}{4\alpha_s^2} + \frac{1}{\rho_0^2} + \frac{k^2 \alpha_s^2}{4L^2} \right)} \tag{5}$$

In the absence of turbulence, the wavefront of the laser beam is not distorted, and thus, the spatial coherence is not affected. To find the received optical intensity in free space (i.e., without turbulence), coherence length in Eq. (4) is chosen as infinite $\rho_0 \rightarrow \infty$, and therefore, Eq. (5) reduces to Eq. (52) of chapter 4 of [33] which is

$$I_0 = \frac{A_s^2 \left(\frac{k\alpha_s}{2L} \right)^2}{\left(\frac{1}{4\alpha_s^2} + \frac{k^2 \alpha_s^2}{4L^2} \right)} = A_s^2 \frac{1}{\Theta_0^2 + \Lambda_0^2} \tag{6}$$

where $\Theta_0 = 1 - L/F_0$, $\Lambda_0 = L/(k\alpha_s^2)$ are the transmitter plane parameters of the Gaussian beam, and $\Theta_0 = 1$ corresponds to the collimated Gaussian beam.

2.2.2 Scintillation index

Scintillation is described as the fluctuations in the received intensity, and the normalized variance of intensity fluctuations is called scintillation index. Under weak intensity fluctuations, the scintillation index is approximately equal to the log-irradiance variance, $\sigma_{\ln I}^2$. Using the Rytov theory and assuming Gaussian beam propagation, $\sigma_{\ln I}^2$ is expressed in terms of the log amplitude variance σ_χ^2 [33] as follows:

$$\sigma_{\ln I}^2 = 4\sigma_\chi^2 = 8\pi^2 k^2 L \int_0^1 \int_0^\infty d\xi \kappa d\kappa \Phi(\kappa) \exp \left(-\frac{\Lambda_1 L \kappa^2 \xi^2}{k} \right) \left\{ 1 - \cos \left[\frac{L \kappa^2 \xi}{k} (1 - \bar{\Theta}_1 \xi) \right] \right\}, \tag{7}$$

where z is distance parameter, $\xi = 1 - z/L$, $\Lambda_1 = \Lambda_0 / (\Theta_0^2 + \Lambda_0^2)$, $\bar{\Theta}_1 = 1 - \Theta_1$, $\Theta_1 = \Theta_0 / (\Theta_0^2 + \Lambda_0^2)$.

It is imperative to emphasize that the performance of UOWC is significantly hindered by the scintillation induced by oceanic turbulence. In the underwater medium, oceanic turbulence is primarily generated by changes in temperature and salinity. As the laser beam propagates through turbulence, owing to random alterations in temperature and salinity, the wavefront of the laser beam is distorted, resulting in fluctuations in received intensity, commonly known as scintillation. The spatial diversity employed in this study serves to hinder the effects of scintillation, thereby enhancing the performance of UOWC links through the utilization of multiple separated small aperture detectors.

2.3 Signal noise in underwater

There are many sources of noise, namely, background noise resulting from ambient light in underwater, thermal noise, shot noise in the presence of received signal, and photodiode dark current noise. These noises degrade the performance of the OWC system in underwater. The total noise variance is defined as the combination of the aforementioned noises and is given by [34]

$$\sigma^2 = \sigma_{Bg}^2 + \sigma_{th}^2 + \sigma_{sn}^2 + \sigma_{dc}^2 \tag{8}$$

where $\sigma_{Bg}^2 = 2qR_pP_{Bg}B_f$ is the background noise variance, $q = 1.60217662 \times 10^{-19}$ is the electronic charge in Coulomb, R_p is the responsivity of the PIN photodetector, P_{Bg} is the background noise power in watts, B_f is the post-detection electrical filter bandwidth in Hz, $\sigma_{th}^2 = 4k_B T_e F_N B_f / R_L$ is the thermal noise variance, $k_B = 1.3807 \times 10^{-23}$ is the Boltzmann’s constant in Joules per degree Kelvin, T_e is the equivalent temperature in degrees Kelvin (°K), F_N is the noise factor of the system, R_L is the equivalent load resistor in ohm, $\sigma_{sn}^2 = 2qR_p \langle I \rangle B_f$ is the shot-noise variance, $\langle I \rangle$ is the received signal power given in Eq. (5), $\sigma_{dc}^2 = 2qI_{dc}B_f$ is the dark current noise, and I_{dc} in Amp is the dark current of the photodiode.

2.4 BER performance of receiver diversity system in log-normal channels

2.4.1 Equal gain combining

EGC system samples each receiver photodetector coherently with equal weights. The sum of irradiances, having statistically independent signal fades causes a decrease in the system noise. Note that the sum of irradiances with equal weights confirms the log-normal distribution. BER of an

optical wireless communication system employing EGC, and BPSK subcarrier intensity modulation is defined by [35]

$$P_{e(EGC)} = \frac{1}{\sqrt{\pi}} \sum_{j=1}^n w_j Q \left[K_1 \exp \left(x_j \sqrt{2\sigma_U^2} + \mu_U \right) \right] \tag{9}$$

where $[w_j]_{j=1}^n$ and $[x_j]_{j=1}^n$, whose values are found in [35], are the weight factors and the zeros of an n-th-order Hermite polynomial, $Q(x) = 0.5 \operatorname{erfc}(x/\sqrt{2})$, $\operatorname{erfc}(\cdot)$ is the complementary error function, $K_1 = R_p I_0 A_s / \sqrt{2N^2 \sigma^2}$, I_0 is the received intensity in the absence of turbulence given in Eq. (6), $\sigma_U^2 = \ln \{ 1 + [\exp(\sigma_{lnI}^2) - 1] / N \}$, σ_{lnI}^2 is the variance of log irradiance, N is the number of separated photodetectors, and $\mu_U = \ln(N) - \frac{1}{2} \sigma_U^2$.

2.4.2 Maximum ratio combining

MRC is an effective combining scheme for receiver arrays to combat underwater turbulence and optical noise. MRC requires estimation of the received irradiance and phase at each branch on the array. Weighted branches with signal, having statistically independent signal fades, are co-phased and summed coherently, and thus, the overall noise in the system is attenuated. BER of an OWC system employing MRC and BPSK subcarrier intensity modulation is given by [35]

$$P_{e(MRC)} = \frac{1}{\pi} \int_0^{\pi/2} [S(\theta)]^N d\theta \tag{10}$$

where

$$S(\theta) \approx \frac{1}{\sqrt{\pi}} \sum_{j=1}^n w_j \exp \left\{ -\frac{K_0^2}{2 \sin^2 \theta} \exp \left[2 \left(x_j \sqrt{2\sigma_{lnI}^2} - \frac{\sigma_{lnI}^2}{2} \right) \right] \right\} \tag{11}$$

and $K_0 = R_p I_0 A_s / \sqrt{2N \sigma^2}$.

2.4.3 Selection combining

In SelC technique, combiner selects the branch that has the strongest SNR level, i.e., probably exposed to less signal fade, and therefore, SNR level at each branch is estimated and compared relatively. In addition, SelC requires only one of the branches, which makes the complexity of the system remarkably reduced compared to EGC and MRC. The

unconditional BER for an OWC system employing SelC and BPSK subcarrier intensity modulation is defined by [35]

$$P_{e(SelC)} = \frac{N}{2^{N-1} \sqrt{\pi}} \sum_{j=1}^n w_j [1 + \operatorname{erf}(x_j)]^{N-1} Q \left[K_0 \exp \left(x_j \sqrt{2\sigma_{\ln I}^2} - \sigma_{\ln I}^2 / 2 \right) \right] \quad (12)$$

3 Numerical results

In this section, the effects of the receiver diversity on the BER performance of an OWC system employing a BPSK modulated Gaussian beam and operating in weak oceanic turbulence are investigated. In the simulation, we focus on the variations of BER performances of an OWC system that employs SelC, EGC, and MRC techniques under various oceanic turbulence conditions. In the

following simulations, a number of the system parameters are assumed to be constant throughout the analysis. The fixed system parameters kept in the simulation are the dark current of the photodiode, $I_{dc} = 10$ nm, the equivalent tem-

perature, $T_e = 300^\circ\text{K}$, the field amplitude of the Gaussian laser $A_s = 30$ mV / m, and the Kolmogorov microscale length $\eta = 1$ mm.

In Fig. 1, the variations of BER versus the number of photodetectors, N , are illustrated for various receiver diversity techniques. Note that $N=1$ means no receiver diversity system, and thus, the BER performances of MRC, EGC, and the SelC are found to be the same. It is observed that an increase in N causes a clear improvement

Fig. 1 Bit error rate versus number of photodetectors N for SelC, EGC, and MRC in oceanic turbulence

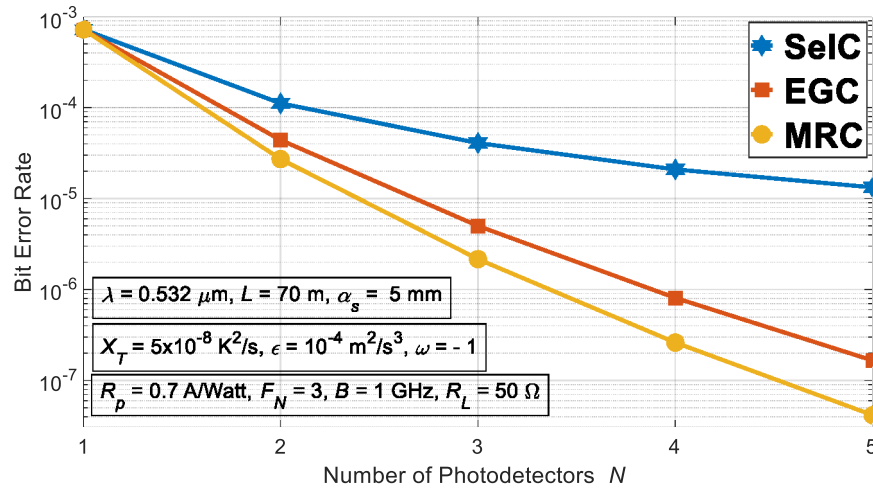
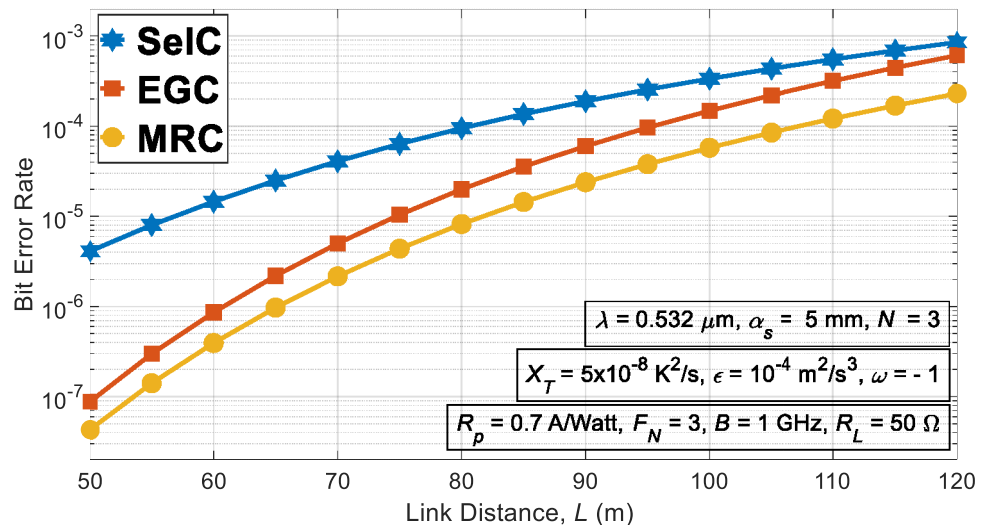


Fig. 2 Bit error rate versus link distance L for SelC, EGC, and MRC



in the system performance because BER decreases rapidly with increasing N . The BER performance of MRC technique is found to be the best compared to that of EGC and the SelC techniques, and it is also found that the performance of EGC is close to the performance of MRC.

In Fig. 2, we aimed at demonstrating the effect of link distance and the receiver diversity techniques on the BER performance of an OWC system in oceanic turbulence. It is clearly seen that at link distance $L = 50$ m, the performance of the SelC combining technique differs from the performance of EGC and MRC techniques. However, with increasing link length, which means increasing turbulence level, BER performance of SelC begins to get closer to BER performances of EGC and MRC. It can be deduced from Fig. 2 that BER performances of EGC and MRC are greater than that of SelC in weaker oceanic turbulence levels but get closer at relatively higher oceanic turbulence levels.

Figure 3 shows the relation between the BER and the ratio of temperature to salinity contributions to the refractive

index spectrum, ω for various receiver diversity techniques. It is observed that, BER performances decrease rapidly with increasing ω causing turbulence level to increase. A similar behavior presented in Fig. 2 is observed in Fig. 3. With increasing ω , the turbulence level increases, and the BER performances of SelC, EGC, and MRC get closer. At $\omega = -5$, a very weak oceanic turbulence level is achieved, and thus, the BER performance of the SelC combining technique becomes quite poor compared to that of EGC and MRC techniques. Figure 3 depicts a closer examination of the details at $\omega = -3$, uncovering that the BER values for SelC, EGC, and MRC are 8.4×10^{-7} , 3.1×10^{-9} , and 1.7×10^{-9} , respectively.

In Fig. 4, we illustrate the BER versus the rate of dissipation of kinetic energy per unit mass of fluid ϵ for various receiver diversity techniques. Note that the oceanic turbulence level decreases gradually with increasing ϵ causing clear performance differences among receiver diversity techniques. When ϵ increases, BER decreases resulting in performance improvement. It can be clearly seen that the BER

Fig. 3 Bit error rate versus ratio of temperature to salinity contributions to the refractive index spectrum ω for SelC, EGC, and MRC

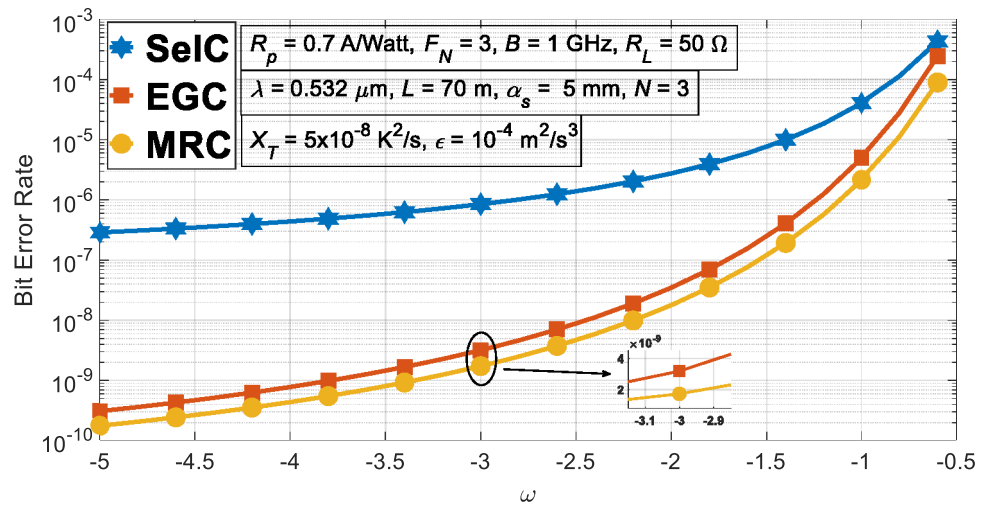


Fig. 4 Bit error rate versus rate of dissipation of kinetic energy per unit mass of fluid ϵ for SelC, EGC, and MRC

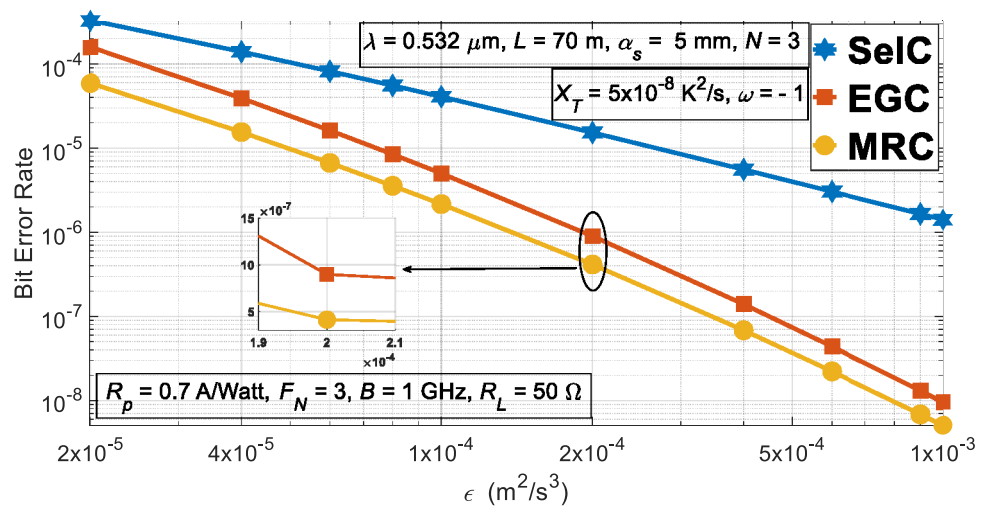
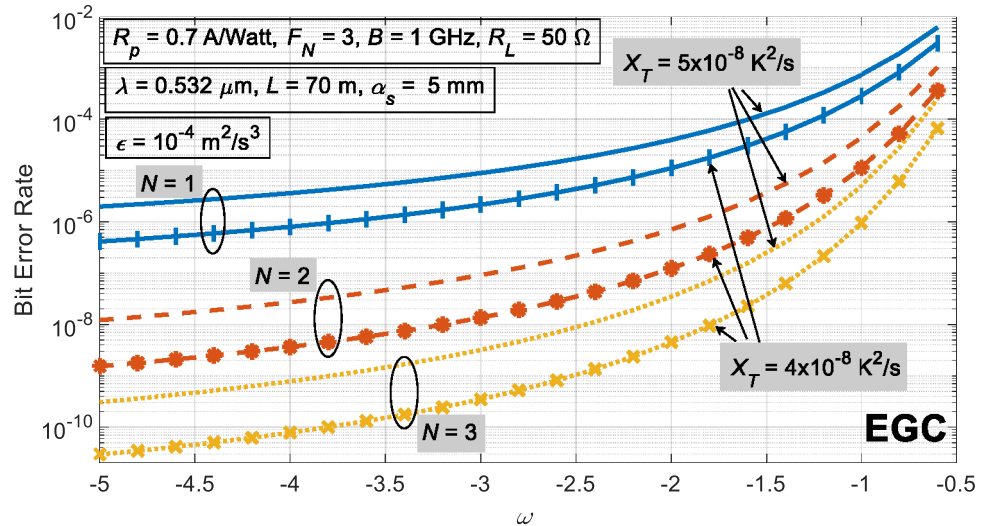


Fig. 5 Bit error rate versus ratio of temperature to salinity contributions to the refractive index spectrum ω for EGC and various N and X_T values



performance of MRC is the best compared to that of EGC and SelC for any ϵ value. The performance of EGC is close to that of MRC but BER values of EGC are slightly higher and lie above the BER values of MRC. The performance of SelC is lower for higher values of ϵ , i.e., at lower oceanic turbulence levels. Figure 4 depicts a closer examination of the details at $\epsilon = 2 \times 10^{-4} \text{m}^2/\text{s}^3$, uncovering that the BER values for SelC, EGC, and MRC are 1.5×10^{-5} , 8.9×10^{-7} , and 4.1×10^{-7} , respectively.

Figure 5 shows BER versus the ratio of temperature to salinity contributions to the refractive index spectrum, ω for EGC, and various N and X_T values. General behavior depicted in Fig. 5 is similar to that in Fig. 3, as ω increases, BER increases. Furthermore, an increase in the number of photodetectors, N apparently improves the BER performance. However, when the rate of dissipation of mean-squared temperature X_T increases, BER performance decreases. It is found that a very large amount of

BER reduction is achieved by using EGC with larger N and at lower values of X_T .

In Fig. 6, we demonstrate how oceanic turbulence and the number of photodetectors influence the BER of an OWC system employing EGC. General trend observed in Fig. 6 is similar to that in Fig. 4 for the variations of ϵ . It is found that EGC with larger N substantially improves the system performance. At a fixed ϵ , a decrease in ω causes the OWC BER performance to increase.

Finally, in Fig. 7, the effects of the noise factor F_N and the responsivity of the PIN photodetector R_p on the BER performance are investigated for an OWC system employing EGC at the receiver. It is found that an increase in N causes an increase in the system performance. At a fixed N , BER performance increases rapidly by reducing F_N and increasing R_p . The physical behavior of this tendency is that when R_p increases, more electrical output improving SNR is obtained, and a decrease in F_N similarly will boost the

Fig. 6 Bit error rate versus rate of dissipation of kinetic energy per unit mass of fluid ϵ for EGC and various ω and N values

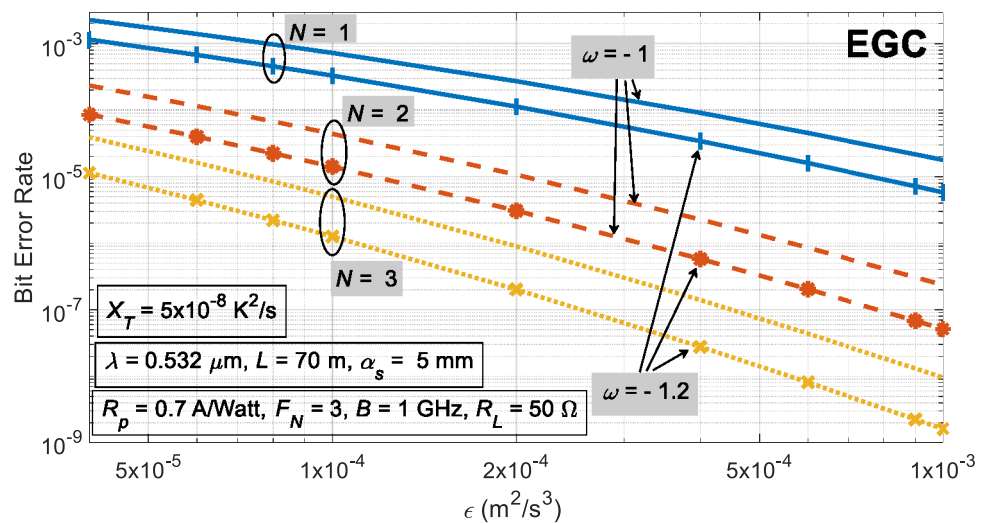
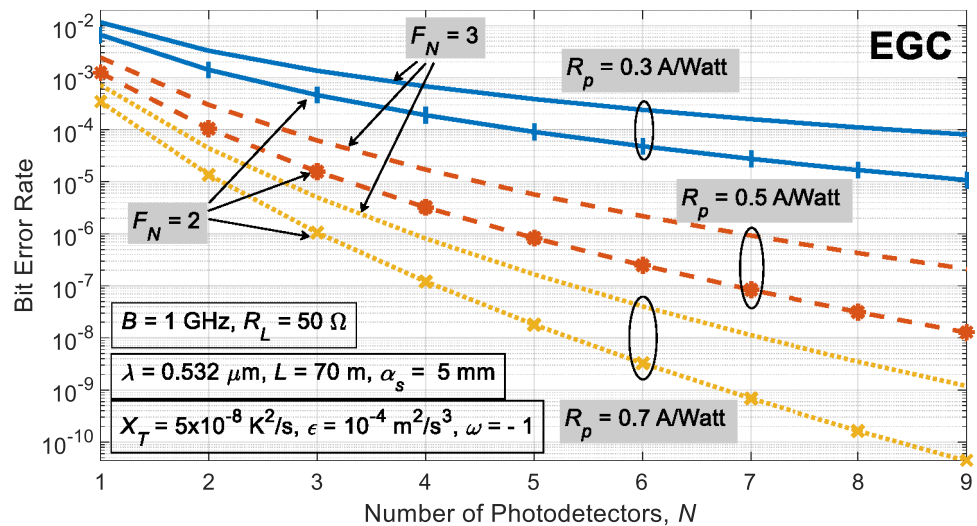


Fig. 7 Bit error rate versus number of photodetectors N for EGC and various F_N and R_p values



SNR of the system which, in turn, result in the improved BER performance.

4 Conclusion

In this study, we investigate how the receiver spatial diversity will boost the BER performance of the OWC system employing a BPSK modulated Gaussian beam and operating in weak oceanic turbulence. The receiver spatial diversity systems considered in this study are the selection combining, equal gain combining, and the maximum ratio combining. The underwater noise sources considered in the simulations are the background noise, thermal noise, shot noise, and the photodiode dark current noise. The turbulence-induced optical intensity on the axis of the photodetector is found by using the extended Huygens–Fresnel principle and is assumed to obey log-normal distribution. On the other hand, the turbulence-induced scintillation index on the axis of the photodetector is derived by using the Rytov method. It is found that as the number of photodetectors, N increases, BER rapidly decreases. Furthermore, an increase in the link distance L , ω , and X_T , causing turbulence level to increase, always result in performance degradation in the OWC system, whereas an increase in ϵ will boost the system performance. BER performance of MRC is found to be the best when compared to that of EGC and SelC at any oceanic turbulence level. The performance of EGC is always between the performance of MRC and SelC but is generally closer to that of MRC. In relatively lower oceanic turbulence levels, SelC shows quite poor BER performance compared to the performances of EGC and MRC. However, when the oceanic turbulence increases, BER performance of SelC begins to get closer to BER performances of EGC and MRC. BER performance of the OWC system increases

rapidly by reducing the noise factor F_N and by increasing the responsivity of the PIN photodetector R_p . EGC technique with higher N and R_p values and with lower F_N value are preferable because of higher BER performance.

The findings in this paper will help OWC system researchers to identify how receiver spatial diversity affects the BER performance of an OWC system that operates in an environment where underwater oceanic turbulence is an active phenomenon.

Acknowledgements M C Gökçe, Y Baykal, and Y Ata acknowledge the support provided by TED University, Çankaya University, and Ostim Technical University, respectively.

Author contributions Muhsin Caner Gökçe: Writing, Investigation, Formal analysis, Software, Original Draft. Yahya Baykal: Writing, Review & Editing, Analytical Derivations, Investigation, Formal analysis. Yalçın Ata: Writing, Review & Editing, Analytical Derivations, Investigation, Formal analysis.

Funding No funding is received by the authors.

Data availability The data that support the findings of this study are available upon reasonable request from the authors.

Declarations

Conflict of Interests The authors declare that there are no conflicts of interest related to this article. The authors declare that they have no known competing financial interests or personal relationships that could have appeared to influence the work reported in this paper.

References

- Zeng, Z., Fu, S., Zhang, H., Dong, Y., Cheng, J.: A survey of underwater optical wireless communications. *IEEE Commun. Surv. Tutor.* **19**(1), 204–238 (2017). <https://doi.org/10.1109/COMST.2016.2618841>

2. Kaushal, H., Kaddoum, G.: Underwater optical wireless communication. *IEEE Access* **4**, 1518–1547 (2016). <https://doi.org/10.1109/ACCESS.2016.2552538>
3. Al-Halafi, A., Oubei, H.M., Ooi, B.S., Shihada, B.: Real-time video transmission over different underwater wireless optical channels using a directly modulated 520 nm laser diode. *IEEE/OSA J. Opt. Commun. Netw.* **9**(10), 826–832 (2017). <https://doi.org/10.1364/JOCN.9.000826>
4. Spagnolo, G.S., Cozzella, L., Leccese, F.: Underwater optical wireless communications: overview. *Sensors* **20**(8), 2261 (2020). <https://doi.org/10.3390/s20082261>
5. Duntley, S.Q.: Light in the sea. *J. Opt. Soc. Am. A* **53**(2), 214–233 (1963). <https://doi.org/10.1364/JOSA.53.000214>
6. Wang, Z., Lu, L., Zhang, P., Qiao, C., Zhang, J., Fan, C., Ji, X.: Laser beam propagation through oceanic turbulence. *IntechOpen* (2018). <https://doi.org/10.5772/intechopen.76894>
7. Korotkova, O., Farwell, N., Shchepakina, E.: Light scintillation in oceanic turbulence. *Wave Random Complex* **22**(2), 260–266 (2012). <https://doi.org/10.1080/17455030.2012.656731>
8. Gökçe, M.C., Baykal, Y.: Aperture averaging and BER for Gaussian beam in underwater oceanic turbulence. *Opt. Commun.* **410**(5), 830–835 (2018). <https://doi.org/10.1016/j.optcom.2017.11.049>
9. Ata, Y., Baykal, Y.: Scintillations of optical plane and spherical waves in underwater turbulence. *J. Opt. Soc. Am. A* **31**(7), 1552–1556 (2014). <https://doi.org/10.1364/JOSAA.31.001552>
10. Gerçekcioğlu, H.: Bit error rate of focused Gaussian beams in weak oceanic turbulence. *J. Opt. Soc. Am. A* **31**(9), 1963–1968 (2014). <https://doi.org/10.1364/JOSAA.31.001963>
11. Nikishov, V.V., Nikishov, V.I.: Spectrum of turbulent fluctuations of the sea-water refraction index. *Int. J. Fluid Mech. Res.* **27**(1), 82–98 (2000). <https://doi.org/10.1615/InterJFluidMechRes.v27.i1.70>
12. Baykal, Y.: Adaptive optics correction of scintillation in underwater medium. *J. Mod. Opt.* **67**(3), 220–225 (2020). <https://doi.org/10.1080/09500340.2019.1710299>
13. Gökçe, M.C., Baykal, Y., Ata, Y.: Adaptive optics effect on performance of BPSK-SIM oceanic optical wireless communication systems with aperture averaging in weak turbulence. *J. Quant. Spectrosc. Radiat. Transfer* **256**, 107335 (2020). <https://doi.org/10.1016/j.jqsrt.2020.107335>
14. Korotkova, O.: Light propagation in a turbulent ocean. *Progress Optics* **64**(1), 1–43 (2019). <https://doi.org/10.1016/bs.po.2018.09.001>
15. Baykal, Y., Gökçe, M.C., Ata, Y.: Anisotropy effect on performance of subcarrier intensity modulated binary phase shift keying optical wireless communication links in weakly turbulent underwater channel. *J. Mod. Opt.* **66**(19), 1871–1875 (2019). <https://doi.org/10.1080/09500340.2019.1682208>
16. Gökçe, M.C., Baykal, Y., Ata, Y.: Binary phase shift keying-subcarrier intensity modulation performance in weak oceanic turbulence. *Phys. Commun.* **37**, 100904 (2019). <https://doi.org/10.1016/j.phycom.2019.100904>
17. Jiang, H., Qiu, H., He, N., Popoola, W., Ahmad, Z., Rajbhandari, S.: Performance of spatial diversity DCO-OFDM in a weak turbulence underwater visible light communication channel. *J. Lightw. Technol.* **38**(8), 2271–2277 (2020). <https://doi.org/10.1109/JLT.2019.2963752>
18. Hema, R., Sudha, S., Aarthi, K.: Performance studies of MIMO based DCO-OFDM in underwater wireless optical communication systems. *J. Mar. Sci. Technol.* **26**, 97–107 (2020). <https://doi.org/10.1007/s00773-020-00724-7>
19. Ramavath, P.N., Udupi, S.A., Krishnan, P.: High-speed and reliable underwater wireless optical communication system using multiple-input multiple-output and channel coding techniques for IoUT applications. *Optics Commun.* **461**, 125229 (2020). <https://doi.org/10.1016/j.optcom.2019.125229>
20. Jamali, M.V., Nabavi, P., Salehi, J.A.: MIMO underwater visible light communications: comprehensive channel study, performance analysis, and multiple-symbol detection. *IEEE Trans. Veh. Technol.* **67**(9), 8223–8237 (2018). <https://doi.org/10.1109/TVT.2018.2840505>
21. Jamali, M.V., Salehi, J.A., Akhoundi, F.: Performance studies of underwater wireless optical communication systems with spatial diversity: MIMO scheme. *IEEE Trans. Commun.* **65**(3), 1176–1192 (2017). <https://doi.org/10.1109/TCOMM.2016.2642943>
22. Liu, W., Xu, Z., Yang, L.: SIMO detection schemes for underwater optical wireless communication under turbulence. *Photon. Res.* **3**(3), 48–53 (2015). <https://doi.org/10.1364/PRJ.3.000048>
23. Peppas, K.P., Boucouvalas, A.C., Ghassemloy, Z.: Performance of underwater optical wireless communication with multi-pulse pulse-position modulation receivers and spatial diversity. *IET Optoelectron.* **11**(5), 180–185 (2017). <https://doi.org/10.1049/iet-opt.2016.0130>
24. Song, Y., Lu, W., Suna, B., Hong, Y., Qu, F., Han, J., Zhang, W., Xu, J.: Experimental demonstration of MIMO-OFDM underwater wireless optical communication. *Optics Commun.* **403**, 205–210 (2017). <https://doi.org/10.1016/j.optcom.2017.07.051>
25. Gökçe, M.C., Baykal, Y.: Scintillation analysis of multiple-input single-output underwater optical links. *J. Opt. Soc. Am. A* **55**(22), 6130–6136 (2016). <https://doi.org/10.1364/AO.55.006130>
26. Liu, W., Jiang, W., Huang, N., Xu, Z.: Experimental investigation of underwater optical wireless communication for correlated simo channel under temperature-induced turbulence. *IEEE Photonics J.* **15**(4), 1–7 (2023). <https://doi.org/10.1109/JPHOT.2023.3289797>
27. Lin, Z., Xu, G., Zhang, Q., Song, Z.: Average symbol error probability and channel capacity of the underwater wireless optical communication systems over oceanic turbulence with pointing error impairments. *Opt. Express* **30**(9), 15327–15343 (2022). <https://doi.org/10.1364/OE.457043>
28. Boluda-Ruiz, R., Salcedo-Serrano, P., Castillo-Vázquez, B., García-Zambrana, A., Garrido-Balsells, J.M.: Capacity of underwater optical wireless communication systems over salinity-induced oceanic turbulence channels with ISI. *Opt. Express* **29**(15), 23142–23158 (2021). <https://doi.org/10.1364/OE.430200>
29. Huang, Y., Zhang, B., Gao, Z., Zhao, G., Duan, Z.: Evolution behavior of Gaussian Schell-model vortex beams propagating through oceanic turbulence. *Opt. Express* **22**(15), 17723–17734 (2014). <https://doi.org/10.1364/OE.22.017723>
30. Cheng, M., Guo, L., Li, J., Zhang, Y.: Channel capacity of the OAM-based free-space optical communication links with Bessel-Gauss beams in turbulent ocean. *IEEE Photon. J.* **8**(1), 7901411 (2016). <https://doi.org/10.1109/JPHOT.2016.2518865>
31. Gradshteyn, S., Ryzhik, I.M.: Tables of integrals, series and products. *Academic* (2000). <https://doi.org/10.1016/C2010-0-64839-5>
32. Wang, S.J., Baykal, Y., Plonus, M.A.: Receiver aperture averaging effects for the intensity fluctuation of a beam wave in the turbulent atmosphere. *J. Opt. Soc. Am.* **73**(6), 831–837 (1983). <https://doi.org/10.1364/JOSA.73.000831>
33. Andrews, L.C., Phillips, R.L.: Laser beam propagation through random media, SPIE, Bellingham. Washington (2005). <https://doi.org/10.1117/3.626196>
34. Jaruwatanadilok, S.: Underwater wireless optical communication channel modeling and performance evaluation using vector radiative transfer theory. *IEEE J. Sel. Areas Commun.* **26**(9), 1620–1627 (2008). <https://doi.org/10.1109/JSAC.2008.081202>
35. Ghassemlooy, Z., Popoola, W., Rajbhandari, S.: Optical wireless communications: system and channel modelling with MATLAB™, Boca Raton, Florida, USA. CRC Press (2012). <https://doi.org/10.1201/b12687>

Publisher's Note Springer Nature remains neutral with regard to jurisdictional claims in published maps and institutional affiliations.

Springer Nature or its licensor (e.g. a society or other partner) holds exclusive rights to this article under a publishing agreement with the author(s) or other rightsholder(s); author self-archiving of the accepted manuscript version of this article is solely governed by the terms of such publishing agreement and applicable law.



Muhsin Caner Gökçe received the M.S. degree in Electronics Engineering from Ankara University, Ankara, Turkey, in 2012, and the Ph.D. degree in Electronic and Communication Engineering from Çankaya University, Ankara, Turkey, in 2016. He is an Associate Professor with the Department of Electrical-Electronics Engineering, TED University, Ankara, Turkey. He is currently employed as a Postdoctoral Researcher in the

Department of Geoscience and Remote Sensing at Delft University of Technology, The Netherlands. His research interests include optical wireless communication and optical beam propagation through turbulent media.



Yahya Baykal received the Ph.D. degree from the Department of Electrical Engineering and Computer Sciences, Northwestern University, Evanston, IL, USA. He is currently a Professor and the Chairman with the Department of Electrical-Electronics Engineering, Çankaya University, Ankara, Turkey. He is the author of more than 225 SCI papers and more than total 300 publications. His research interests include optical wave prop-

agation in atmospheric and underwater media.



Yalçın Ata (Senior Member, IEEE) received the Ph.D. degree in Electrical and Electronics Engineering from Gazi University, Ankara, Türkiye, in 2010. From 2004 to 2020, he was a Senior Researcher, a Chief Researcher, and the Deputy Director of the TUBITAK Defense Industries Research and Development Institute and the TUBITAK Space Technologies Research Institute, Ankara, Türkiye, respectively. He is currently a Full Professor with the Electrical and Electronics Engineering

Department, OSTİM Technical University, Ankara. His research interests include optical wireless communication, free-space optics, quantum communication, optical turbulence in atmosphere, underwater and biological tissue, and beam propagation in turbulent media.